Single histidine button in cardiac troponin I sustains heart performance in response to severe hypercapnic respiratory acidosis *in vivo*

Nathan J. Palpant,* Louis G. D'Alecy,* and Joseph M. Metzger[†,1]

*Department of Molecular and Integrative Physiology, University of Michigan Medical School, Ann Arbor, Michigan, USA; and [†]Department of Integrative Biology and Physiology, University of Minnesota Medical School, Minneapolis, Minnesota, USA

ABSTRACT **Intracellular acidosis is a profound negative regulator of myocardial performance. We hypothesized that titrating myofilament calcium sensitivity by a single histidine substituted cardiac troponin I (A164H) would protect the whole animal physiological response to acidosis *in vivo*. To experimentally induce severe hypercapnic acidosis, mice were exposed to a 40% CO_2 challenge. By echocardiography, it was found that systolic function and ventricular geometry were maintained in cTnI A164H transgenic (Tg) mice. By contrast, non-Tg (Ntg) littermates experienced rapid and marked cardiac decompensation during this same challenge. For detailed hemodymanic assessment, Millar pressure-conductance catheterization was performed while animals were treated with a β-blocker, esmolol, during a severe hypercapnic acidosis challenge. Survival and load-independent measures of contractility were significantly greater in Tg *vs.* Ntg mice. This assay showed that Ntg mice had 100% mortality within 5 min of acidosis. By contrast, systolic and diastolic function were protected in Tg mice during acidosis, and they had 100% survival. This study shows that, independent of any β-adrenergic compensation, myofilament-based molecular manipulation of inotropy by histidine-modified troponin I maintains cardiac inotropic and lusitropic performance and markedly improves survival during severe acidosis *in vivo*.—Palpant, N. J., D'Alecy, L. G., Metzger, J. M. Single histidine button in cardiac troponin I sustains heart performance in response to severe hypercapnic respiratory acidosis *in vivo*. *FASEB J.* 23, 1529–1540 (2009)**

Key Words: myocardial function · myofilaments · pH

Acute heart failure can result from myocardial acidosis. Myocardial acidosis arises from reduced plasma oxygen tension (hypoxic acidosis), as in cases of myocardial ischemia (1, 2), or accumulated levels of plasma carbon dioxide (hypercapnic acidosis or hypercarbia), found with severe pulmonary diseases such as chronic obstructive pulmonary disease (COPD) (3) or emphysema (4). Acidosis has numerous pathophysiological implications within the context of many organ systems, including significant deleterious effects on the contractile function of the heart (5–9). Homeostasis is tightly regulated in the heart, which makes this organ particularly sensitive to whole-animal metabolic changes and the downstream influence on pH status and energy availability (10, 11).

There are numerous changes that occur in the heart under conditions of acidosis, including altered excitation-contraction coupling (8, 10, 12–15). The present study focused on altered sarcomeric protein function known to significantly reduce cardiac contractility during acute acidosis independent of altered Ca^{2+} handling (6, 16, 17). A key regulator of myofibrillar contraction is the troponin complex, including the calcium binding subunit, troponin C (TnC), and the inhibitory subunit, troponin I (TnI). Calcium increases the TnI-TnC interaction, causing these subunits to act as a dynamic switch within the myofilament during systole and diastole. Acidosis diminishes myofilament Ca^{2+} sensitivity, due in part to reduced Ca^{2+} binding to troponin C (6, 18), and impaired interactions between TnI and TnC during systole. Thus, this complex serves as a key regulator of beat-to-beat contractility in the heart (19). In the whole heart, this reduction in myofilament Ca^{2+} sensitivity is a key contributor to the reduction in acute myofilament force production and a consequent decrement in left ventricular developed pressure *in vivo* (20, 21).

Earlier biochemical studies established that neonatal myocardium is more resilient to low pH (7), a phenotype correlated with fetal expression of the slow skeletal isoform of TnI. The ssTnI isoform is better able to retain proper myofibrillar contractility during acidosis (22–29). Specifically, the pCa ($-\log[Ca^{2+}]$) required for 50% activation of myofilaments in adult cardiac myocytes, which express the adult isoform of TnI (cTnI), drops by more than 1 pCa units during acidification of pH (from

[1] Correspondence: Department of Integrative Biology and Physiology, University of Minnesota Medical School, 6-125 Jackson Hall, 321 Church St. SE, Minneapolis, MN 55455, USA. E-mail: metzgerj@umn.edu

doi: 10.1096/fj.08-121996

pH 7.0 to 6.2). This is compared to adult myocytes transduced with an adenoviral construct expressing the slow skeletal isoform of TnI (ssTnI), which show an attenuated pCa shift during acidification of pH (from pH 7.0 to 6.2) (24). Several studies have further demonstrated that the unique biochemistry of ssTnI can be reproduced in the adult TnI isoform (cardiac TnI) by substituting a single histidine residue for alanine at codon 164 (27–31). This modification is located at the interface between TnC and actin binding domains involved in the switch function of TnI. We have generated a murine transgenic mouse model wherein this histidine button has been engineered into the adult cardiac isoform of TnI (cTnI A164H) under control of the α-myosin heavy-chain promoter. This provides a biophysical basis for a functional molecular rheostat of intracellular pH in the adult heart (9, 20). Cellular data have shown that myocytes expressing cTnI A164H have intact responses to isoproterenol and PKA by hastening relaxation kinetics and shifting the tension-pCa relationship (20). Furthermore, calcium load is diminished in these myocytes, which is manifest in a lower calcium transient amplitude (20, 32). Studies of transgenic (Tg) mice expressing this engineered mutant cTnI show improved cardiac inotropic function in response to a variety of pathophysiological challenges, including acute and chronic ischemia (20), as well as in a mouse model of age-induced cardiomyopathy (32).

The current study focused exclusively on the *in vivo* whole animal response to acidosis in the context of this modified cTnI using an experimental model of severe respiratory hypercapnia. A major aim of this study was to block adrenergic support in the heart and subsequently analyze cardiac function *in vivo* under baseline conditions and during exposure to acidosis. Adrenergic stimulation is a major regulator of cardiac function at baseline in the rodent (20, 22). Furthermore, high sympathetic stimulation of rodent hearts at baseline has been shown to compensate and mask cardiomyopathic phenotypes that are revealed during suppression of catecholamine signaling (33). In light of this, β-blockade in mouse models consisting of myofilament modifications (20, 34, 35) is of particular importance for determining any functional aberrations caused by altered myofilament calcium responsiveness on systolic and diastolic performance. Furthermore, β-blockade allows for the functional readout of intrinsic inotropic performance of the heart *in vivo*, which is important in determining the potential for cardiac contractile responsiveness to injury. These questions have not been addressed in the cTnI A164H Tg mouse to date. The new findings of this study show that cTnI A164H preserves systolic and diastolic performance during acidosis *in vivo*. This study suggests that the biochemical function of cTnI A164H as a molecular rheostat in the sarcomere may protect cardiac performance in a range of pathologies associated with acidosis.

MATERIALS AND METHODS

Mouse model

Generation and analysis of Tg mice expressing a histidine-modified cardiac troponin I (cTnI A164H) with FLAG epitope were previously described (20). The procedures used in this study are in agreement with the guidelines of the University of Michigan and approved by the University of Michigan Committee on the Use and Care of Animals. Veterinary care was provided by the University of Michigan Unit for Laboratory Animal Medicine. The University of Michigan is accredited by the American Association of Accreditation of Laboratory Animal Health Care, and the animal care use program conforms to the standards of the U.S. National Institutes of Health (NIH) Guide for the Care and Use of Laboratory Animals (NIH Pub. No. 85–23).

Conductance micromanometry

Measurements of *in vivo* cardiovascular hemodynamics were obtained using conductance micromanometry, as previously performed by this laboratory (20). Mice were anesthetized and ventilated *via* a tracheal cannulation and ventilated *via* a pressure-controlled ventilator with 1% isoflurane at a peak inspiratory pressure of 15 cm H_2O and a respiratory rate of 60 breaths/min. With the aid of a dissecting microscope, the heart was exposed *via* a thoracotomy. A 1.4 French Millar pressure-volume catheter (PVR-1045; Millar Instruments, Houston, TX, USA) was then placed into the left ventricular chamber *via* an apical stab. Left ventricular pressure and volume measurements were collected at a sampling rate of 1 kHz. Data were analyzed with Ponemah software, P3 Plus (DSI International, St. Paul, MN, USA). Transient inferior vena cava (IVC) occlusions were also performed to obtain the end-systolic and end-diastolic pressure-volume relationships. IVC occlusions were performed at baseline and at 5 min of esmolol infusion (**Fig. 3*a***). After obtaining baseline hemodynamics (ventilated with isoflurane and O_2), mice received a continuous infusion of esmolol (250 μg/kg/min) that continued until the completion of the assay. After 5 min of esmolol infusion, mice were exposed to an acute hypercapnic acidosis challenge (40% CO_2 balanced with oxygen) (for schematic diagram of protocol, see Supplemental Fig. 3). Data were acquired until systolic failure, which was defined as the point when peak left ventricular systolic pressure dropped to 50 mmHg. At this point, esmolol infusion was stopped, and mice were revived using 100% O_2 in order to obtain instrument calibration.

Echocardiography

Anesthesia was induced with 3% isoflurane and then maintained at 1% for the duration of the procedure. The hair was removed from the upper abdominal and thoracic area with depilatory cream. Electrocardiography (ECG) was monitored *via* noninvasive resting ECG electrodes. Transthoracic echocardiography was performed in the supine or left lateral position. Two-dimensional, M-mode, Doppler, and tissue Doppler echocardiographic images were recorded using a VisualSonics' Vevo 770 high-resolution *in vivo* microimaging system (VisualSonics Inc., Toronto, ON, Canada). The systolic and diastolic dimensions and wall thickness were measured in M mode in the parasternal short-axis view at the level of the papillary muscles (36, 37). Fractional shortening and ejection frac-

tion were calculated from the M-mode parasternal short-axis view (37). Diastolic function was assessed by conventional pulsed-wave spectral Doppler analysis of mitral valve inflow patterns [early (E) and late (A) filling waves]. Doppler tissue imaging (DTI) was used to measure the early (E_a) and late (A_a) diastolic tissue velocities of the lateral annulus. As a combined measure of systolic and diastolic function, the TEI index was measured as $(LV_{ctetrt}-LV_{et})/LV_{ctetrt}$, in which LV_{ctetrt} is the total time of left ventricular contraction, ejection plus relaxation and LV_{et} is left ventricular ejection time. After acquiring baseline echocardiographic data, mice were exposed to a hypercapnic acidosis challenge (ventilation with 40% CO_2 balanced with oxygen) for 10 min. During ventilation with CO_2, efforts were taken to confirm that the nose and mouth were within the nose cone to prevent any dilution of the inhaled gas due to gasping of room air. Data were acquired every 2.5 min for the duration of the challenge. All mice survived this challenge and were returned to their cage for recovery.

In vivo arterial pressure and ECG telemetry

Implantable radiotelemetry probes (C-10 implants; DSI International, St. Paul, MN, USA) for measurement of real-time systemic blood pressure and ECG in freely moving unanesthetized animals was accomplished, as described previously (38–40). One week after implantation of telemetry probe, mice were placed in a flow-through chamber initially flushed with room air (20.93% O_2), allowing rodents time to equilibrate to the new environment. They were then exposed to a hypercapnic acidosis challenge (40 min exposure to 40% CO_2 balanced with oxygen). On completion of the challenge, mice were removed from the chamber and returned to their cage for recovery.

Blood gas analysis

Mice were anesthetized with 1% isoflurane and exposed to a hypercapnic acidosis challenge (40% CO_2 balanced with oxygen) for 10 min without external ventilator support. A second cohort of Tg mice was also exposed to a hypercapnic acidosis challenge for 20 min. During ventilation with CO_2, efforts were taken to confirm that the nose and mouth were within the nose cone to prevent any dilution of the inhaled gas due to gasping of room air. At the end of the challenge the thoracic cavity was opened to expose the heart. Approximately 600 μl of oxygenated blood was drawn from the left ventricle and immediately analyzed using a Radiometer ABL505 blood gas analyzer (Radiometer, Westlake, OH, USA).

Statistics

All results are expressed as means ± SE. All single variable assays were assessed by two-tailed *t* test. All multivariable assays were assessed using either one-way analysis of variance (ANOVA) or two-way repeated-measures ANOVA with Tukey *post hoc* test. Survival after the *in vivo* acute hypercapnic acidosis challenge was assessed by the Fisher exact test.

RESULTS

Echocardiography assessment during acute respiratory hypercapnic acidosis

Using echocardiography to track *in vivo* left ventricular function, Tg mice retained global cardiac performance and proper left ventricular dimensions during exposure to acidosis. By contrast, nontransgenic (Ntg) mice showed significant myocardial contractile dysfunction throughout the same challenge (**Fig. 1**). In addition to the summarized echo data (Fig. 1*b, c*), **Table 1** shows changes in cardiac function at the end of the challenge compared to measurements taken at the beginning and at the nadir for each parameter. We found that the function of Tg hearts at the end of the challenge was not significantly different from baseline based on a repeated-measures one-way ANOVA. In contrast, the lowest point of function for Ntg mice was at the end of the challenge in all cases, or the nadir to the end of the challenge was not significant from 0 based on a Dunnet's test.

In addition to being mildly hypercontractile at baseline, echocardiography data showed evidence of a modest decrease during the early stages of the acidosis challenge, which reverted by the 10-min time point in Tg mice. At the end of the challenge, aspects of Tg heart performance were not significantly different from baseline [*e.g.*, Tg ejection fraction (EF) at baseline: 75.1±4.7 *vs.* 68.1±5.7% after 10 min of acidosis; NS] (Fig. 1*b, c*). By contrast, Ntg mice showed a significant reduction in cardiac contractility throughout the challenge (*e.g.*, EF at 10 min of acidosis: 23.6±4.9 *vs.* 67.8±4.5% for Ntg and Tg; $P<0.05$) (Fig. 1*b, c*; Supplemental Fig. 1). Furthermore, Tg mice retained ventricular geometry during the hypercapnic acidosis challenge compared to Ntg mice that underwent significant left ventricular cavitary dilation (*e.g.*, LV dimensions at systole at 10 min of acidosis: 17.3±1.2 *vs.* 9.3±1.3 mm for Ntg and Tg; $P<0.05$) (Fig. 1*b, c*). As a measure of diastolic function, the mitral valve inflow velocity (MV E), measured by Doppler, recovered to baseline function after the nadir in Tg mice compared to Ntg mice, in which compromised diastolic function persisted throughout the acidosis challenge (MV E change from nadir to end in Tg mice: 262.5±81.7 mm/s) (Table 1). Lastly, as an assessment of overall diastolic and systolic function, the TEI index indicated that Tg mice underwent an initial phase of cardiac decompensation during the onset of acidosis but were able to recover function by the end of the challenge compared to Ntg mice, which showed persistent cardiac dysfunction throughout the hypercapnic acidosis challenge (TEI index at 10 min of acidosis: 0.62±0.05 *vs.* 0.5±0.03 for Ntg and Tg; $P<0.05$) (Supplemental Fig. 1). All mice recovered from this hypercapnic acidosis challenge.

Blood gas analysis during acidosis

To assess whether there were any differences in blood gas parameters during the acidosis challenge, arterial blood gases were analyzed during hypercapnic acidosis. These data indicate that, although significantly different from baseline values, blood gases taken at 10 min of exposure to 40% CO_2 were not different between Tg and Ntg mice

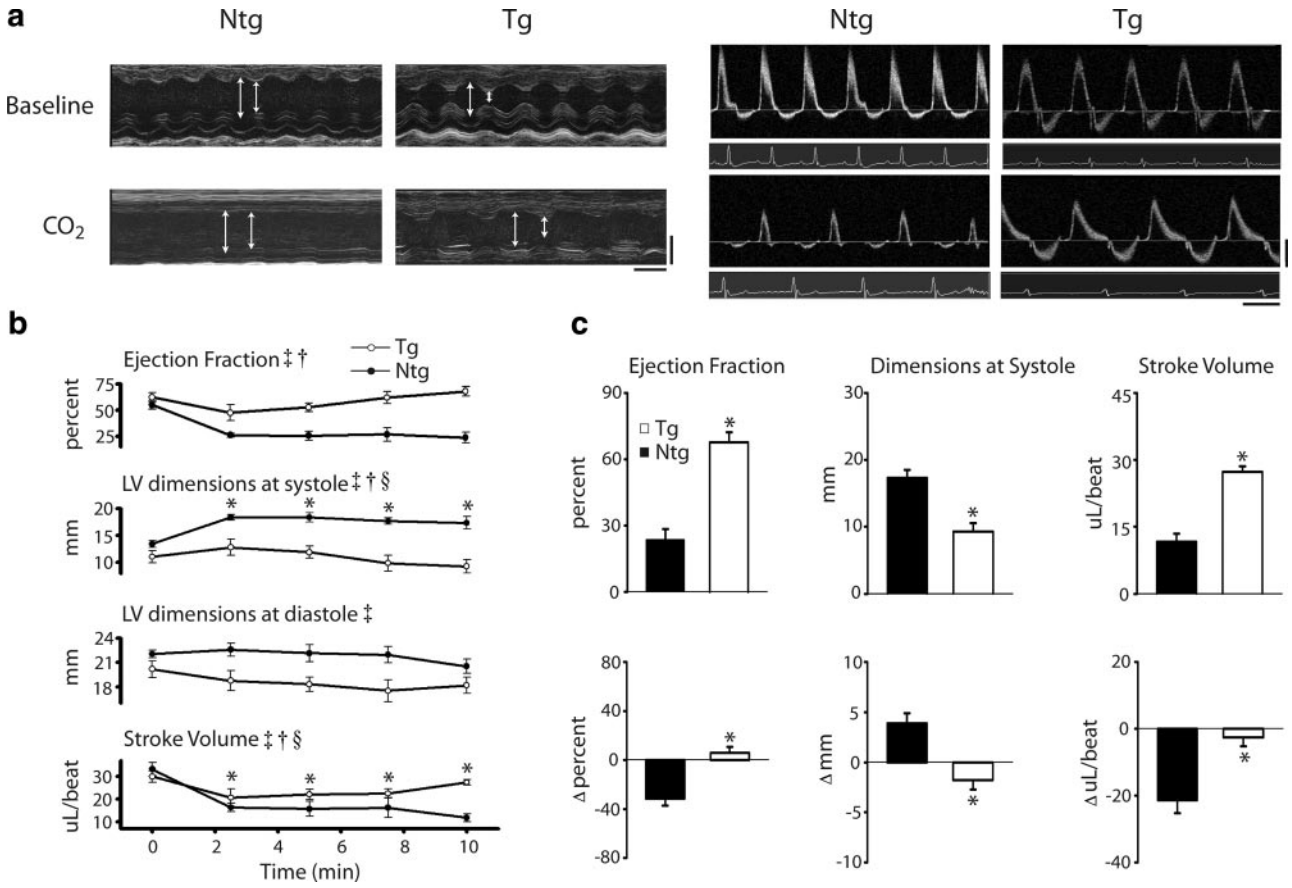

Figure 1. Cardiac function assessed by echocardiography at baseline and during acidosis. *a*) Left panels: representative M-mode echocardiographic images along the parasternal short-axis view showing changes in contractility of Ntg and Tg mice at baseline and after 10 min of exposure to 40% CO_2. White bars delineate systole and diastole. Time bar = 100 ms; distance bar = 2 mm. Right panels: representative conventional pulsed-wave spectral Doppler analysis of mitral valve inflow and aortic valve outflow patterns at baseline and after 10 min of exposure to 40% CO_2 in Ntg and Tg mice. Time bar = 100 ms; flow rate bar = 40 cm/s. *b*) Summarized mean data showing changes in cardiac functional parameters, including ejection fraction, left ventricular (LV) dimensions at systole and diastole, and stroke volume between Ntg (●) and Tg (○) mice during the time course of hypercapnic acidosis. *c*) Mean data showing the difference in ejection fraction, LV dimensions at systole, and stroke volume after 10 min exposure to 40% CO_2 (top) as well as the change (Δ) in function from baseline (bottom) in Ntg (■) and Tg (□) mice. Values are expressed as means ± SE. Two-way repeated-measures ANOVA main effects: $^{\ddagger}P < 0.05$ for time; $^{\dagger}P < 0.05$ for genotype. Two-way repeated measures ANOVA interaction effects: $^{\S}P < 0.05$ for time *vs.* genotype; *P < 0.05 for Ntg *vs.* Tg. Ntg, $n = 5$; Tg, n = 7.

(**Table 2**). In both Tg and Ntg mice, blood pH decreased from 7.2 at baseline to below 6.63 during the hypercapnic challenge, demonstrating the development of significant acidemia. This is consistent with changes in pCO_2 which increased from baseline values at 55 to 60 mmHg to >250 mmHg during acidosis in both Tg and Ntg animals. This increase in carbon dioxide was also confirmed in measures of total plasma CO_2 that were significantly increased during the hypercapnic challenge. Although oxygen availability during acidosis was increased from room air values (60% compared to ~21%, respectively), oxygen saturation tended to decrease from baseline values of 102% to below 88% during hypercapnia, although this trend did not reach statistical significance for either group. Lastly, plasma concentrations of titratable base (SBE_c) were significantly reduced ($P<0.05$) during hypercapnia compared to baseline values, which is consistent with acidemia. There were no significant changes in plasma bicarbonate during ventilation with 40% CO_2, indicating that these mice were not experiencing metabolic acidosis.

Blood gas analysis was also performed on Tg mice after 20 min of exposure to 40% CO_2. Changes in pH indicate that the blood continued to acidify to a degree significantly lower than the pH reached after 10 min of hypercapnic acidosis (serum pH 6.62±0.02 *vs.* 6.55±0.00 at 10 and 20 min; $P<0.05$). Furthermore, SBE_c continued to decrease concomitant with the decrease in blood pH. These findings are consistent with the development of an increasingly severe respiratory hypercapnic acidemia. However, even at 20 min exposure to 40% CO_2, plasma bicarbonate remained steady, indicating the absence of any metabolic acidosis.

Blood pressure and ECG telemetry *in vivo* during hypercapnic acidosis challenge

In vivo continuous arterial pressure telemetry of freely moving unanesthetized animals was carried out between Ntg and Tg mice. Furthermore, this study ana-

TABLE 1. *Changes in cardiac function during acidosis*

Parameter	Baseline	Nadir	End	Nadir to end
Echocardiography				
Tg				
EF (%)	62.2 ± 4.4	47.4 ± 7.6$^{\#}$	67.8 ± 4.5†	20.4 ± 4.8*
Vol s (μl)	19.7 ± 3.3	24.4 ± 4.9$^{\#}$	14.4 ± 3.4†	−10.1 ± 2.9*
TEI index	0.4 ± 0.03	0.6 ± 0.04$^{\#}$	0.5 ± 0.03†,‡	−0.1 ± 0.0*
MV E (mm/s)	883.8 ± 24.4	541.1 ± 63.0$^{\#}$	803.6 ± 36.6†	262.5 ± 81.7*
Ntg				
EF (%)	55.0 ± 4.1	23.6 ± 4.9$^{\#}$	23.6 ± 4.9‡	0.0 ± 0.0
Vol s (μl)	27.0 ± 2.6	45.8 ± 2.4$^{\#}$	40.6 ± 5.1‡	−5.1 ± 5.9
TEI index	0.40 ± 0.02	0.65 ± 0.03$^{\#}$	0.62 ± 0.05‡	−0.03 ± 0.07
MV E (mm/s)	1069.7 ± 57.1	646.6 ± 146.7$^{\#}$	646.6 ± 146.7‡	0.0 ± 0.0
Hemodynamics				
Tg				
CI (+*dP/dt*/mmHg)	196.9 ± 9.6	113.1 ± 2.4$^{\#}$	126.4 ± 6.7‡	12.2 ± 6.5*
Max vol (μl)	27.3 ± 4.1	36.3 ± 5.0$^{\#}$	32.5 ± 5.0‡	−3.8 ± 1.2*
EDp (mmHg)	6.2 ± 1.1	12.3 ± 1.8$^{\#}$	7.9 ± 1.8†	−4.4 ± 0.8*
E_a (ESp/SV)	5.4 ± 0.6	8.4 ± 0.4$^{\#}$	6.2 ± 0.7†	−2.2 ± 0.6*
Ntg				
CI (+*dP/dt*/mmHg)	169.0 ± 26.6	95.7 ± 5.7$^{\#}$	0.0 ± 0.0	—
Max vol (μl)	28.1 ± 5.4	55.1 ± 5.5$^{\#}$	0.0 ± 0.0	—
EDp (mmHg)	4.0 ± 1.0	10.8 ± 1.7$^{\#}$	0.0 ± 0.0	—
Ea (ESp/SV)	6.2 ± 0.4	14.2 ± 2.5$^{\#}$	0.0 ± 0.0	—

Analysis of cardiac function during acidosis in Tg and Ntg mice showing changes between baseline, nadir (worst value for a given parameter), and end of challenge. All values are expressed as means ± SE. Echocardiographic parameters: ejection fraction (EF), volume at systole (vol s), TEI index, and inflow velocity of mitral valve E wave (MV E). Tg, $n = 7$; Ntg, $n = 5$. Hemodynamic parameters: contractility index (CI), left ventricular maximum volume (max vol), end diastolic pressure (EDp), and arterial elastance (E_a). Tg, $n = 7$; Ntg, $n = 6$. *$P < 0.05$ *vs.* a hypothetical zero; Dunnets one-sample *t* test with Wilcoxon signed-rank *post hoc.* $^{\#}P < 0.05$ *vs.* baseline, $^{\dagger}P < 0.05$ *vs.* nadir, $^{\ddagger}P < 0.05$ vs. baseline; repeated-measures one-way ANOVA.

lyzed the extent to which cTnI A164H mice were able to maintain systemic perfusion pressures during a prolonged hypercapnic acidosis challenge (40 min exposure to 40% CO_2) compared to Ntg littermates (**Fig. 2**). At baseline, circadian rhythms showed changes in blood pressure over 24 h indicating that Ntg mice had increased systolic blood pressure compared to Tg mice ($P<0.05$). However, diastolic arterial pressure was not different between groups. Furthermore, these telemetered data showed that Ntg mice also had a higher baseline heart rate than Tg mice (472.2±15.6 *vs.* 555.4±18.7 for Tg and Ntg; $P<0.05$) (Fig. 2*a, b*).

After 1 wk of baseline blood pressure measurements, mice were exposed to a 40-min hypercapnic acidosis challenge. The change in arterial systolic pressure between baseline (average daytime systolic pressure) and the initial exposure to high flow 40% CO_2 indicated that both Ntg and Tg mice had a significant increase in blood pressure in response to this challenge (Fig. 2*c, d*). This can be attributed as an indirect measure of whole animal adrenergic stimulation during this challenge in both groups. Furthermore, cTnI A164H mice had significantly higher systolic and diastolic arterial pressures during the acidosis challenge compared to Ntg littermates (*e.g.*, ΔMAP −81.5±18.4 *vs.* −37.7±6.3 mmHg for Ntg and Tg; $P<0.05$) (Fig. 2*c, e,* and *F*).

TABLE 2. *Arterial blood gas analysis*

Parameter	Ntg baseline	Ntg CO_2 (10 min)	Tg baseline	Tg CO_2 (10 min)	Tg CO_2 (20 min)
pH	7.2 ± 0.02	6.61 ± 0.01*	7.2 ± 0.0	6.62 ± 0.02$^{\#}$	6.55 ± 0.0†,‡
pCO_2 (mmHg)	55.3 ± 1.8	258.6 ± 13.6*	59.1 ± 2.9	265.7 ± 8.5$^{\#}$	277.3 ± 14.5‡
pO_2 (mmHg)	383.6 ± 69.6	196.9 ± 43.9	296.8 ± 60.4	206.5 ± 38.7	301.0 ± 15.2
sO_2 (%)	102.9 ± 1.0	87.7 ± 5.1	102.4 ± 1.0	86.2 ± 6.4	94.9 ± 3.6
HCO_3^- (mM)	23.5 ± 0.7	24.4 ± 0.9	23.1 ± 1.1	25.8 ± 0.6	23.2 ± 0.5
tCO_2 (vol %)	56.5 ± 1.6	72.5 ± 2.7*	55.6 ± 2.6	76.0 ± 1.4$^{\#}$	71.5 ± 1.9‡
SBE_c (mMl)	−2.8 ± 0.9	−13.4 ± 0.7*	−3.6 ± 0.9	−12.1 ± 0.8$^{\#}$	−15.7 ± 0.3†,‡

All values are expressed as means ± SE. pCO_2, partial pressure of carbon dioxide; pO_2, partial pressure of oxygen; sO_2, plasma oxygen saturation (fraction of oxyhemoglobin in deoxy-plus oxyhemoglobin of blood); HCO_3^-, bicarbonate; tCO_2, total plasma carbon dioxide of whole blood; SBE_c, standardized base excess (concentration of titratable base). Ntg baseline, $n = 5$; Tg baseline, $n = 5$; Ntg CO_2 (10 min), $n = 5$; Tg CO_2 (10 min), $n = 6$; Tg CO_2 (20 min), $n = 5$. *$P < 0.05$ vs. Ntg baseline; *t* test. $^{\#}P < 0.05$ *vs.* Tg baseline, $^{\dagger}P < 0.05$ *vs.* Tg CO_2 (10 min), $^{\ddagger}P < 0.05$ *vs.* Tg baseline; one-way ANOVA.

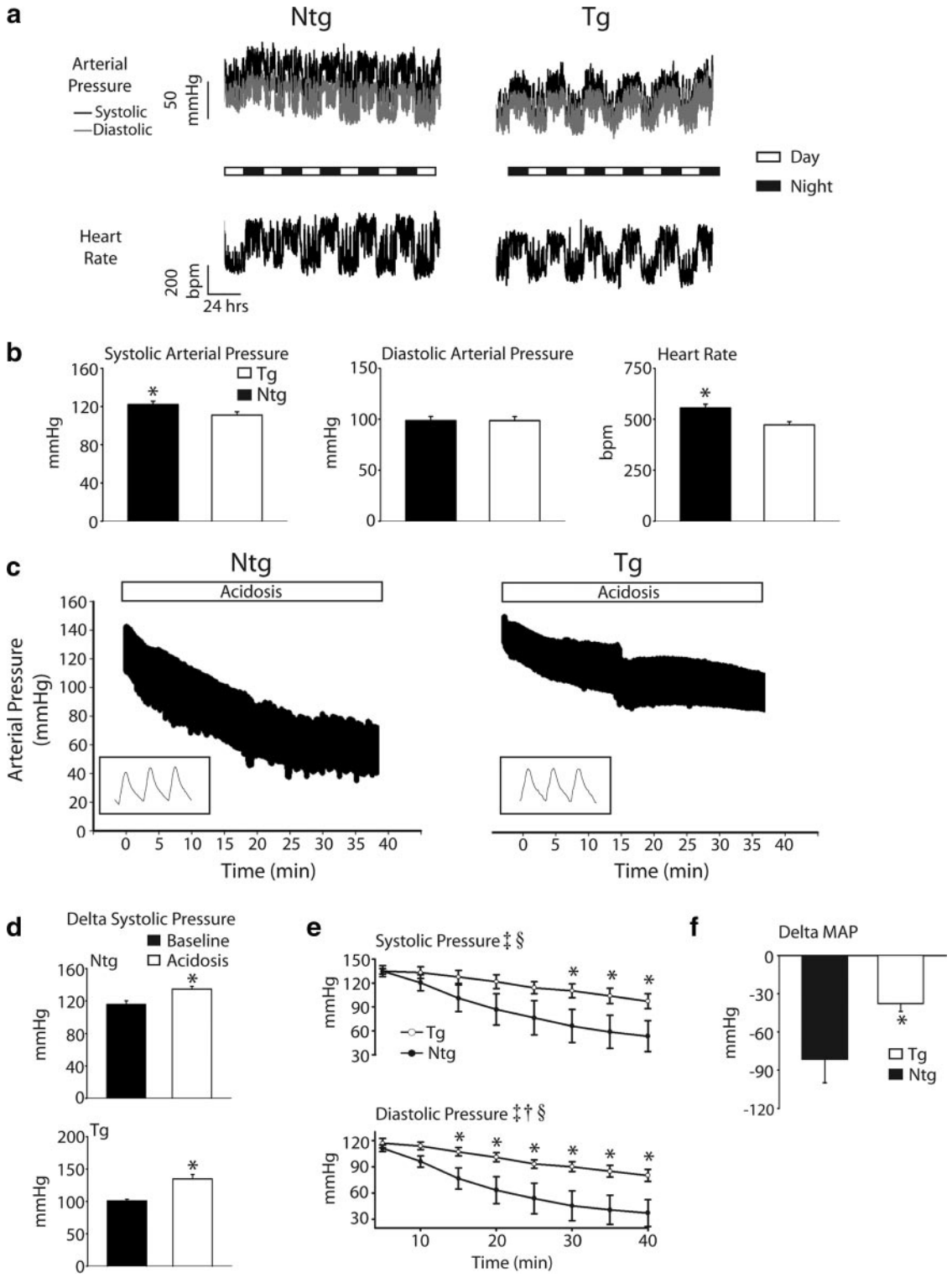

Figure 2. Radiotelemetry-based blood pressure recordings in vivo. *a*) Representative raw arterial pressure and heart rate trace recording baseline circadian rhythms from Ntg and Tg mice over the course of 5 days. *b*) Mean systolic arterial pressure (left), diastolic arterial pressure (middle), and heart rate (right) during a given 24 h of baseline analysis for Ntg (■) and Tg (□) mice. *c*) Representative raw pressure traces during 40 min of exposure to 40% CO_2 for Ntg and Tg mice. *d*) Average change in systolic arterial blood pressure at baseline (■) and at the onset of acidosis (□), illustrating the stress response in both Ntg and Tg mice. *e*) Mean data for systolic and diastolic arterial pressure measurements between nontransgenic (●) and transgenic (○) mice during the time course of hypercapnic acidosis. *f*) Change in mean arterial pressure (MAP) from baseline to the completion of the hypercapnic acidosis challenge for Ntg (■) and Tg (□) mice. Values are expressed as means ± SE. Two-way repeated-measures ANOVA main effects: $^{‡}P < 0.05$ for time; $^{†}P < 0.05$ for genotype. Two-way repeated measures ANOVA interaction effects: $^{§}P < 0.05$ for time *vs.* genotype; *$P < 0.05$ for Ntg *vs.* Tg. Ntg, $n = 4$; Tg, $n = 7$.

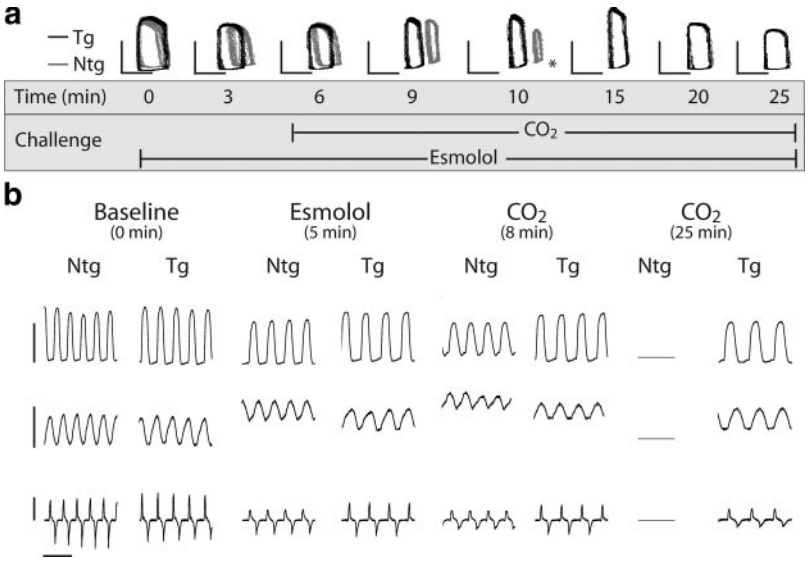

Figure 3. Raw data traces of real-time conductance micromanometry during hypercapnic acidosis. *a*) Representative raw pressure-volume loops (pressure bar=60 mmHg, volume bar=20 μl) of Ntg (gray) and Tg (black) mice during the time course of an esmolol plus hypercapnic acidosis challenge. Asterisk indicates time of death for Ntg mouse. *b*) Representative raw traces of pressure (top; bar=60 mmHg), volume (middle; bar=30 μl), and pressure derivatives (bottom; bar=10,000 mmHg/s) for Ntg and Tg mice at baseline, during infusion of esmolol (5 min), at 8 min into the acidosis challenge, and at the end of the assay (25 min), illustrating changes in cardiac contractility and geometry during the time course of this challenge. Time scale bar = 0.2 s.

To determine whether Tg mice were able to maintain proper sinus rhythm during acidosis, we performed continuous telemetered electrocardiographic measurements during a 40-min hypercapnic acidosis challenge. These data show that both Ntg and Tg mice experienced intermittent extended R-R intervals associated with sinus pause or sinus dysfunction throughout the time course of hypercapnic acidosis (Supplemental Fig. 2). Overall, there was no difference in the frequency or duration of this episodic sinus dysfunction between Ntg and Tg mice during acidosis (Supplemental Fig. 2*b, c*). Furthermore, core body temperature and heart rate decreased similarly between Ntg and Ttg mice during prolonged acidosis (Supplemental Fig. 2*d, e*). All mice recovered from this 40-min hypercapnic acidosis challenge.

Assessment of cardiac function during β-blockade

To directly assess cardiac hemodymanics, mice were surgically instrumented by implantation of a conductance micromanometry catheter into the left ventricle. After stabilization of cardiac function, baseline measurements were acquired followed by an infusion of esmolol (250 μg/kg/min) to suppress adrenergic involvement in the cardiac response to acidosis. Inferior vena cava occlusions (IVCOs) were performed just prior to the start and after 5 min of esmolol infusion to acquire load-independent measures of contractility (For full experimental protocol, see Supplemental Fig. 3). These data show that during the initial 5 min of esmolol infusion, Ntg and Tg mice experienced a slowing of the heart rate, left ventricular cavitary dilation (*e.g.*, increased LV max volume), a slight diminution in measures of contractility (*e.g.*, systolic pressure, $+dP/dt$, contractility index, ejection fraction, and stroke work) and evidence of marked slowing in diastolic function [increased left ventricular end-diastolic pressure (LVEDp) and Tau] (**Figs. 3*a, b* and 4*a***). However, contractile performance was significantly better in cTnIA164H Tg than Ntg mice after 5 min of esmolol infusion based on higher ejection fraction, stroke work, and $+dP/dt$ (*e.g.*, $+dP/dt$ 4603.7±612 *vs.* 7094.1±545 mmHg/s for Ntg and Tg; $P<0.05$) (**Fig. 5*a***). Intrinsic inotropic function measured from the slope of the end-systolic pressure-volume relationship (ESPVR; end-systolic pressure:end-systolic volume) and preload recruitable stroke work (PRSW; stroke work:end-diastolic volume) assessed load-independent measures of contractility (acquired by PV loop analysis during IVCO) (Fig. 5*b*). This analysis showed a higher preload-independent inotropic capacity in Tg mice compared to Ntg mice at baseline and during esmolol infusion. The negative derivative of pressure development ($-dP/dt$, data not shown), end-diastolic pressure (EDp), and Tau were not different between Ntg and Tg mice during esmolol infusion, indicating comparable diastolic function between these groups (Fig. 4*a*).

Cardiac function and survival during hypercapnic acidosis with β-blockade

We next tested the hypothesis that catecholaminergic stimulation played a significant role in the survival capacity of mice during the acute hypercapnic acidosis challenge. To address this, cardiac function was assessed during acute acidosis without endogenous β-adrenergic support. Mice were instrumented with a conductance micromanometry catheter and infused with esmolol for 5 min (as described above) and then exposed to 40% CO_2 for 20 min with the esmolol infusion continuing to the completion of the challenge (Supplemental Fig. 3). By pressure-volume analysis, at the onset of respiratory hypercapnic acidosis, Ntg mice underwent precipitous cardiac decompensation within the first 5 min of acidosis (Figs. 3*a, b*). In terms of inotropic function, this decline in cardiac performance was characterized by a sudden decrease in systolic pressure, ejection frac-

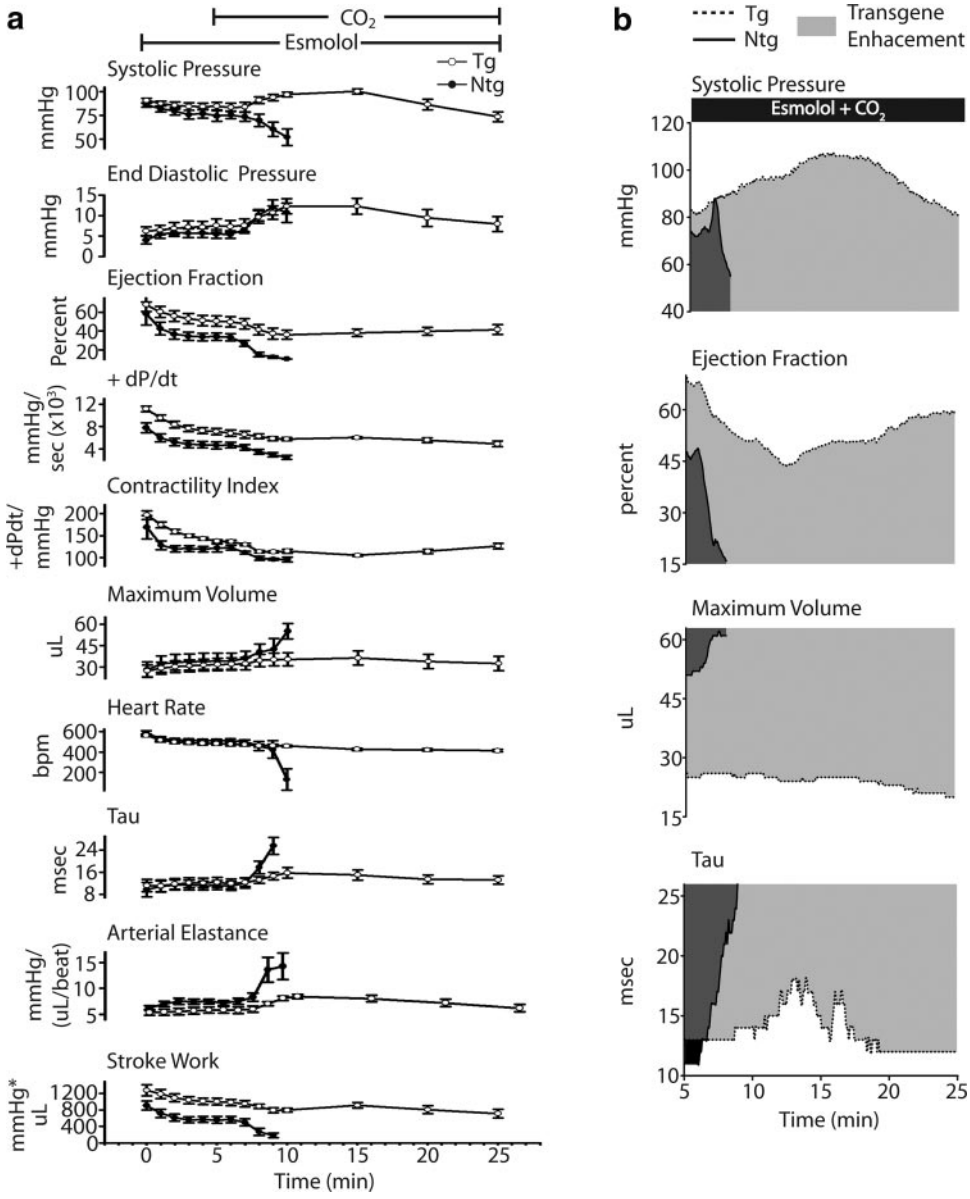

Figure 4. Summary of real-time *in vivo* hemodynamic data. *a*) Summarized mean data showing changes in cardiac functional and geometric parameters, including systolic pressure, end-diastolic pressure, $+dP/dt$, contractility index, ejection fraction, maximum volume, Tau, heart rate, and stroke work between Ntg (●) and Tg (○) mice during the time course of esmolol infusion and acute hypercapnic acidosis. *b*) Representative raw data (derived from 5-s averages) of end-systolic pressure, ejection fraction, maximum volume, and Tau during 20 min of esmolol plus acidosis, showing transgene enhancement (light gray) of cTnI A164H. Values are expressed as means ± SE. Ntg, $n = 6$; Tg, $n = 7$.

tion, contractility index, and stroke work (Figs. 4 and 5*a*). Furthermore, diastolic dysfunction emerged during the onset of acidosis (increased LVEDp and Tau) together with further dilation of left ventricular chamber geometry (Fig. 4).

In marked contrast, Tg mice showed sustained cardiac function during this respiratory hypercapnic acidosis challenge, even in the absence of β-adrenergic support (Fig. 3*a, b*). These data represent a transgene enhancement effect on the part of cTnI A164H mice, which contributes to their survival capacity compared to Ntg mice (Fig. 4*b*). More specifically, Tg mice actually increased their developed pressure, made evident by an immediate increase in end-systolic pressure (ESp) and, more modestly, the positive derivative of pressure development ($+dP/dt$) and stroke work (Fig. 4*a, b* and 5*a*). This was sustained until the latter phases of acidosis, when LVESp decreased to slightly below baseline values together with a drop in the $+dP/dt$ and stroke work (Figs. 4*a, b* and 5*a*).

Other hemodynamic parameters of cardiac function for Tg mice in this group showed an initial decrease during the onset of acidosis followed unexpectedly by a recovery toward baseline values during the latter stages of acidosis (Fig. 4 and Table 1). Similar to the echocardiography data, Table 1 shows the restoration in function at the end of the challenge compared to measurements taken at the beginning and at the nadir for parameters derived by hemodynamic analysis. These measurements reveal that function at the end of the challenge was not significantly different than baseline in Tg mice. During the onset of acidosis, measures of contractility decreased initially but returned toward baseline during the latter phases of acidosis (*e.g.*, from the nadir contractility index increased by 21.1±26.5 U) (Figs. 4*a* and 5*a* and Table 1). The contractility index

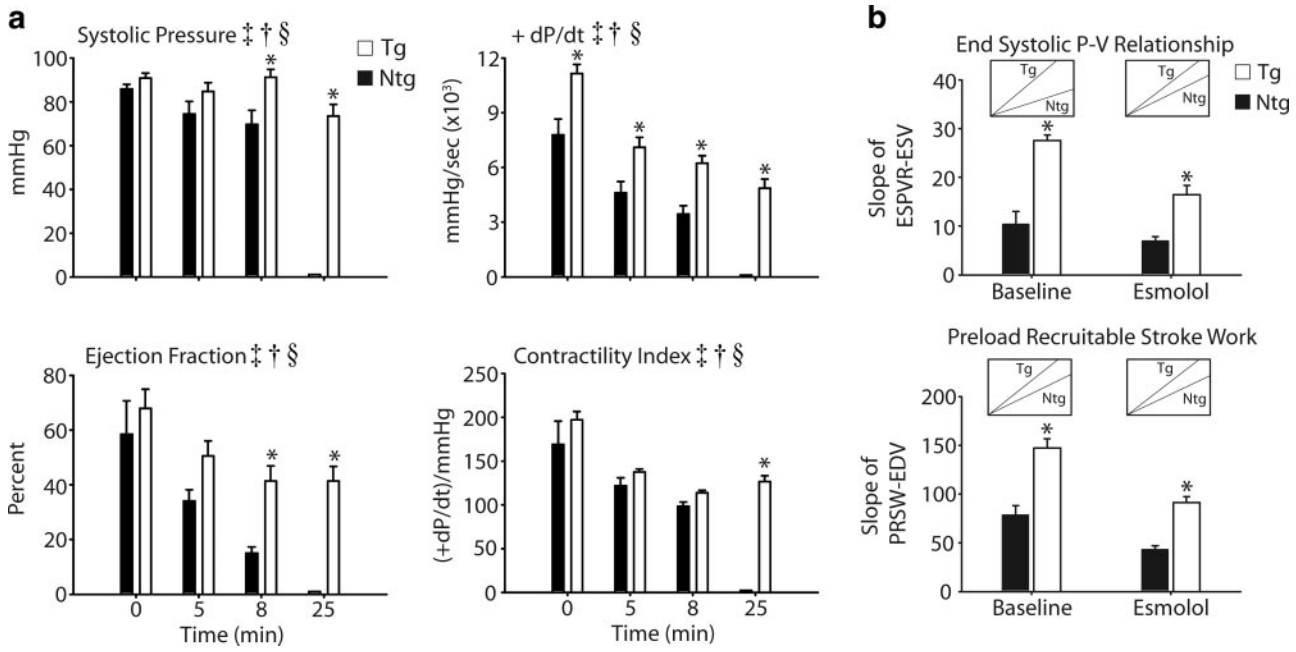

Figure 5. Hemodynamic analysis of inotropic function during esmolol and acidosis. *a*) Mean data extracted at baseline, at 5 min after esmolol infusion, at 8 min into the acidosis challenge, and at the end of the protocol (25 min) showing a significant difference between Ntg (■) and Tg (□) mice based on contractile properties, including systolic pressure, $+dP/dt$, ejection fraction, and contractile index. *b*) Load-independent measures of contractility acquired by IVCOs, including end-systolic pressure volume relationship (ESPVR) and preload recruitable stroke work (PRSW), showing the difference between Ntg (■) and Tg (□) mice at baseline and during infusion of esmolol. Insets: representative slopes for Ntg and Tg mice. Values are expressed as means ± SE. Two-way repeated-measures ANOVA main effects: $^{\ddagger}P < 0.05$ for time; $^{\dagger}P < 0.05$ for genotype. Two-way repeated measures ANOVA interaction effects: $^{\S}P < 0.05$ for time *vs.* genotype; *P < 0.05 for Ntg *vs.* Tg. Ntg, $n = 6$; Tg, $n = 7$.

(CI) is defined as the positive-pressure derivative ($+dP/dt$) normalized to the ventricular pressure at that point. Taking this into consideration, this change in CI is understood as the maintenance of the positive-pressure derivative despite decreases in the ESp during acidosis, suggestive of an overall increase in contractility during this challenge. Diastolic function also increased initially but returned to baseline values by the end of the challenge (*e.g.*, from the nadir LVEDp decreased in Tg mice 4.4±0.8 mmHg) (Fig. 4 and Table 1). Similarly, ventricular dilation occurred at the onset of acidosis followed by a restoration of the ventricular chamber geometry during the latter phases of hypercapnia (*e.g.*, maximum volume decreased from the nadir in Tg mice 3.8±1.2 μl) (Fig. 4*a* and Table 1). In all cases, the absolute change between the nadir and the end of the challenge for parameters given in Table 1 was different from zero based on a Dunnet's analysis, showing a recovery of hemodynamic function during acidosis in Tg mice. However, in stark contrast to the functionality of Tg mice throughout this challenge, the lowest point for Ntg mice was at the time of death (Table 1). When assessed for survival, cTnI A164H mice showed a significant transgene-mediated enhancement of cardiac function, while Ntg mice develop severe cardiac dysfunction and pump failure in response to hypercapnic acidosis with β-adrenergic blockade. The 100% survival of Tg mice compared to 100% failure in Ntg mice within 5 min of the onset of acidosis is a striking indicator of the improved inotropy caused by this single amino acid substitution (**Fig. 6*a, b***).

DISCUSSION

Cardiomyopathies associated with myocardial acidosis can result in profound systolic and diastolic dysfunction. Understanding mechanisms associated with protecting cardiac pump performance during acidosis are important in developing therapies. This study reveals whole animal responses in Tg mice expressing a single histidine modified cardiac TnI during acute respiratory hypercapnic acidosis. During hypercapnia, cTnI A164H mice had a significantly greater capacity to maintain cardiac geometry and function compared to Ntg mice. Furthermore, in the absence of catecholaminergic support, Tg mice showed markedly improved survival *vs.* Ntg mice. This outcome resulted from the ability of Tg mice to maintain significantly higher intrinsic cardiac function without compromising diastolic performance compared to Ntg mice. Among studies seeking to preserve pump function in disease (20, 22, 41), results from the present study show a unique response of improved systolic and diastolic performance during acidosis *in vivo*. Overall, the results of this study illustrate that molecular manipulation of myofilament performance by means of a histidine button engineered

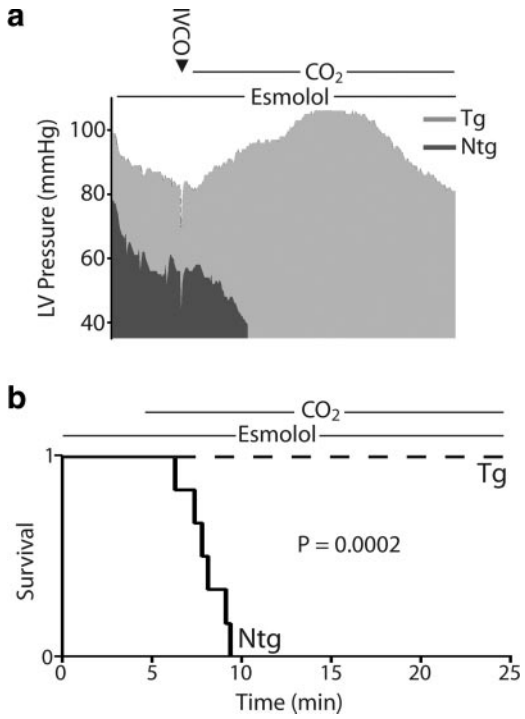

Figure 6. Survival data during respiratory hypercapnic acidosis. *a*) Representative raw data (derived from 5-s averages) for ESp over the full time course of the experimental protocol, including esmolol infusion followed by CO_2 ventilation for Ntg and Tg mice. *b*) Survival curve showing the time of pump failure for Ntg mice, which occurred after the onset of ventilation with 40% CO_2 compared to the 100% survival of Tg mice after 25 min of exposure to this challenge. Ntg, $n = 6$; Tg, $n = 7$.

into the switch region of cTnI results in significant protection of cardiac geometry and function and improved survival in the context of severe respiratory hypercapnic acidosis *in vivo*.

Myofilament calcium sensitivity and acidosis

Elevated plasma CO_2 occurs in numerous pathophysiological contexts, such as severe COPD (42), conditions of hypercarbic respiratory failure (43), respiratory infections (44), or congenital central hypoventilation syndrome (45). A fundamental consequence of decreases in pH is the uncoupling of excitation-contraction (E-C) events, which are necessary for the tight regulation of beat-to-beat pump activity in the heart (5, 46). At the subcellular level, E-C uncoupling is made evident by an acidosis-induced reduction in force-generating capacity by the sarcomere for any given $[Ca^{2+}]_i$. Acidosis decreases both maximal Ca^{2+}-activated tension and the Ca^{2+} sensitivity of tension (2, 20, 23, 31, 32, 47). Acidosis also decreases myocyte maximal sarcomere length shortening amplitude and shortening velocity (20, 48, 49). These experiments illustrate that myofilament Ca^{2+} desensitization at low pH is a fundamental molecular deficiency responsible for cardiac organ pathologies associated with myocardial acidosis (9). Notably, results from this study demonstrate that cTnI A164H works effectively to prevent this Ca^{2+} desensitization and provides a survival benefit to respiratory acidosis in an intact animal model.

Adrenergic blockade and cTnI A164H performance

Sympathetic stimulation increases cardiac inotropy and lusitropy. It has been shown that rodent hearts have high β-adrenergic tone under baseline conditions (20, 22). This may mask cardiomyopathies associated with alterations in myofilament calcium handling (33). Consequently, we addressed the role played by β-adrenergic signaling using a β-blocker, esmolol, during hemodynamic analysis to determine the intrinsic systolic and diastolic properties of the cTnI A164H heart. Notably, we found load-independent measures of contractility were significantly higher in Tg *vs.* Ntg mice under β-blockade, suggesting a higher intrinsic capacity for contractile function in cTnI A164H Tg mice. Hemodynamic measurements obtained in this study demonstrate the first evidence that cTnI A164H mice can maintain cardiac function during acidosis *in vivo*.

Although enhanced systolic function is expected with this model, diastolic function (*e.g.*, Tau, EDp) can be problematic for Tg mouse models expressing altered myofilament proteins. For example, calcium-sensitizing models show diastolic dysfunction, such as cTnI R193H (34), cTnT R92Q (51), and ssTnI mice *in vivo* (35). Notably, this study shows that, in the absence of sympathetic activity, baseline diastolic function of cTnI A164H Tg mice is not different from the Ntg cohort.

cTnI A164H: a titratable myofilament inotrope

Multiple investigators have proposed that targeting myofilament calcium responsiveness *via* manipulation of TnC and TnI interactions is desirable for protecting cardiac function during acidosis (20, 22, 30, 41, 51–53). However, previous approaches have found that enhancement of systolic function often concomitantly results in diastolic dysfunction, as discussed above. For example, Tg mice expressing ssTnI show improved cardiac function during acidosis (22). However, they also show significant diastolic dysfunction during this challenge (22, 35), and more generally, these hearts lack the ability to modulate TnI function *via* PKA activation by β-adrenergic signaling. Pharmacological alterations of the myofilament using TnC Ca^{2+} sensitizers, such as levosimendan, also improve inotropy (41, 54–56) but have significant non-TnC actions. In contrast, the present study shows that cTnI A164H is capable of improving myofilament function in response to acidosis, without concomitant diastolic dysfunction, alterations in β-adrenergic signaling, or nonspecific effects on myocyte function.

The underlying biochemistry of a histidine button engineered into TnI provides insights into potential mechanisms supporting this concept. Specifically, histidine ionizes near physiological pH with a pK_R around

6.0. Consequently, under mildly acidic conditions the increasing propensity for the ionization of histidine changes the biochemical function of surrounding residues and any interactions mediated by this region of the protein. In cardiac troponin I, this histidine substitution (A164H) is positioned in the regulatory domain between the amphiphilic switch region (helix 3) and the C-terminal actin binding domain (helix 4). Previous studies have shown that this region is critically involved in the interaction between TnI and TnC during systole through the electrostatic binding of the switch region of TnI with the calcium-saturated N-terminal hydrophobic patch of TnC (57–61). Although further studies are required to address the specific biophysical consequences of these potential interactions, the physiological implications of this histidine modification have been reported by this and other studies (20). We propose that cTnI A164H acts as a molecular rheostat maintaining systolic and diastolic pump function in models of severe acidosis and ischemic cardiomyopathy *in vitro* and *in vivo*.

This study contributes new evidence that shows a potential therapeutic role of cTnI A164H in the heart. Specifically, evidence from these experiments demonstrates a marked transgene enhancement effect that confers protection from acidosis-induced pump failure and death in living animals. We hypothesize that this response is mediated foremost by the underlying biochemistry of the histidine-modified cTnI acting as a molecular rheostat of the intracellular milieu. This study contributes to the growing evidence that histidine-modified troponin I is an effective target protein for the protection of cardiac performance during severe acidosis *in vivo*. FJ

We thank Dr. Robert Bartlett for generous use of his blood gas analysis machine and Dr. Terry Major for assistance with analysis of blood gas parameters. Drs. Margaret Westfall and Sharlene Day provided invaluable insight into the development of this manuscript. We also thank Steven Whitesall for his assistance with telemetered mice and Kimber Converso for her expert murine echocardiography measurements. This work was supported by grants from the NIH (J.M.) and the American Heart Association (N.P.).

REFERENCES

1. Steg, P. G., Dabbous, O. H., Feldman, L. J., Cohen-Solal, A., Aumont, M. C., Lopez-Sendon, J., Budaj, A., Goldberg, R. J., Klein, W., Anderson, F. A., Jr., for the Global Registry of Acute Coronary Events, I. (2004) Determinants and prognostic impact of heart failure complicating acute coronary syndromes: observations from the Global Registry of Acute Coronary Events (GRACE). *Circulation* **109,** 494–499
2. Godt, R. E., and Nosek, T. M. (1989) Changes of intracellular milieu with fatigue or hypoxia depress contraction of skinned rabbit skeletal and cardiac muscle. *J. Physiol.* **412,** 155–180
3. Windisch, W., Kostic, S., Dreher, M., Virchow, J. C., Jr., and Sorichter, S. (2005) Outcome of patients with stable COPD receiving controlled noninvasive positive pressure ventilation aimed at a maximal reduction of Pa(CO2). *Chest* **128,** 657–662
4. Tsunezuka, Y., Sato, H., Tsubota, M., and Seki, M. (2000) Significance of percutaneous cardiopulmonary bypass support for volume reduction surgery with severe hypercapnia. *Artif. Organs* **24,** 70–73
5. Orchard, C. H., and Kentish, J. C. (1990) Effects of changes of pH on the contractile function of cardiac muscle. *Am. J. Physiol.* **258,** C967–C981
6. Parsons, B., Szczesna, D., Zhao, J., Van Slooten, G., Kerrick, W. G., Putkey, J. A., and Potter, J. D. (1997) The effect of pH on the Ca^{2+} affinity of the Ca^{2+} regulatory sites of skeletal and cardiac troponin C in skinned muscle fibres. *J. Muscle Res. Cell Motil.* **18,** 599–609
7. Solaro, R. J., Lee, J. A., Kentish, J. C., and Allen, D. G. (1988) Effects of acidosis on ventricular muscle from adult and neonatal rats. *Circ. Res.* **63,** 779–787
8. Crampin, E. J., and Smith, N. P. (2006) A dynamic model of excitation-contraction coupling during acidosis in cardiac ventricular myocytes. *Biophys. J.* **90,** 3074–3090
9. Day, S. M., Westfall, M. V., and Metzger, J. M. (2007) Tuning cardiac performance in ischemic heart disease and failure by modulating myofilament function. *J. Mol. Med.* **85,** 911–921
10. Lee, J. A., and Allen, D. G. (1991) Mechanisms of acute ischemic contractile failure of the heart. Role of intracellular calcium. *J. Clin. Invest.* **88,** 361–367
11. Lutgens, E., Daemen, M. J. A. P., de Muinck, E. D., Debets, J., Leenders, P., and Smits, J. F. M. (1999) Chronic myocardial infarction in the mouse: cardiac structural and functional change. *Cardiovasc. Res.* **41,** 586–593
12. Allen, D. G., and Orchard, C. H. (1983) The effects of changes of pH on intracellular calcium transients in mammalian cardiac muscle. *J. Physiol.* **335,** 555–567
13. Del Monte, F., Lebeche, D., Guerrero, J. L., Tsuji, T., Doye, A. A., Gwathmey, J. K., and Hajjar, R. J. (2004) Abrogation of ventricular arrhythmias in a model of ischemia and reperfusion by targeting myocardial calcium cycling. *Proc. Natl. Acad. Sci.* **101,** 5622–5627
14. Koretsune, Y., and Marban, E. (1989) Cell calcium in the pathophysiology of ventricular-fibrillation and in the pathogenesis of postarrhythmic contractile dysfunction. *Circulation* **80,** 369–379
15. Solaro, R. J., el Saleh, S. C., and Kentish, J. C. (1989) Ca^{2+}, pH and the regulation of cardiac myofilament force and ATPase activity. *Mol. Cell. Biochem.* **89,** 163–167
16. Fabiato, A., and Fabiato, F. (1978) Effects of pH on the myofilaments and the sarcoplasmic reticulum of skinned cells from cardiac and skeletal muscles. *J. Physiol.* **276,** 233–255
17. Metzger, J. M. (1995) Myosin binding-induced cooperative activation of the thin filament in cardic myocytes and skeletal muscle fibers. *Biophys. J.* **68,** 1430–1442
18. Ding, X. L., Akella, A. B., Sonnenblick, E. H., Rao, V. G., and Gulati, J. (1996) Molecular basis of depression of Ca^{2+} sensitivity of tension by acid pH in cardiac muscles of the mouse and the rat. *J. Card. Fail.* **2,** 319–326
19. Farah, C. S., and Reinach, F. C. (1995) The troponin complex and regulation of muscle contraction. *FASEB J.* **9,** 755–767
20. Day, S. M., Westfall, M. V., Fomicheva, E. V., Hoyer, K., Yasuda, S., La Cross, N. C., D'Alecy, L. G., Ingwall, J. S., and Metzger, J. M. (2006) Histidine button engineered into cardiac troponin I protects the ischemic and failing heart. *Nat. Med.* **12,** 181–189
21. Metzger, J. M., and Westfall, M. V. (2004) Covalent and noncovalent modification of thin filament action: the essential role of troponin in cardiac muscle regulation. *Circ. Res.* **94,** 146–158
22. Urboniene, D., Dias, F. A. L., Pena, J. R., Walker, L. A., Solaro, R. J., and Wolska, B. M. (2005) Expression of slow skeletal troponin I in adult mouse heart helps to maintain the left ventricular systolic function during respiratory hypercapnia. *Circ. Res.* **97,** 70–77
23. Westfall, M. V., Borton, A. R., Albayya, F. P., and Metzger, J. M. (2002) Myofilament calcium sensitivity and cardiac disease: insights from troponin I isoforms and mutants. *Circ. Res.* **91,** 525–531
24. Westfall, M. V., Rust, E. M., and Metzger, J. M. (1997) Slow skeletal troponin I gene transfer, expression, and myofilament incorporation enhances adult cardiac myocyte contractile function. *Proc. Natl. Acad. Sci.* **94,** 5444–5449
25. Wolska, B. M., Vijayan, K., Arteaga, G. M., Konhilas, J. P., Phillips, R. M., Kim, R., Naya, T., Leiden, J. M., Martin, A. F., de Tombe, P. P., and Solaro, R. J. (2001) Expression of slow skeletal troponin I in adult transgenic mouse heart muscle reduces the force decline observed during acidic conditions. *J. Physiol.* **536,** 863–870

26. Metzger, J. M., Michele, D. E., Rust, E. M., Borton, A. R., and Westfall, M. V. (2003) Sarcomere thin filament regulatory isoforms. Evidence of a dominant effect of slow skeletal troponin I on cardiac contraction. *J. Biol. Chem.* **278,** 13118–13123
27. Westfall, M. V., and Metzger, J. M. (2001) Troponin I isoforms and chimeras: tuning the molecular switch of cardiac contraction. *News Physiol. Sci.* **16,** 278–281
28. Westfall, M. V., and Metzger, J. M. (2003) Gene transfer of troponin I isoforms, mutants, and chimeras. *Adv. Exp. Med. Biol.* **538,** 169–174; discussion 174
29. Westfall, M. V., Albayya, F. P., Turner, I. I., and Metzger, J. M. (2000) Chimera analysis of troponin I domains that influence Ca^{2+}-activated myofilament tension in adult cardiac myocytes. *Circ. Res.* **86,** 470–477
30. Dargis, R., Pearlstone, J. R., Barrette-Ng, I., Edwards, H., and Smillie, L. B. (2002) Single mutation (A162H) in human cardiac troponin I corrects acid pH sensitivity of Ca^{2+}-regulated actomyosin S1 ATPase. *J. Biol. Chem.* **277,** 34662–34665
31. Westfall, M. V., Borton, A. R., Albayya, F. P., and Metzger, J. M. (2001) Specific charge differences in troponin I isoforms influence myofilament Ca^{2+} sensitivity of tension in adult cardiac myocytes. *Biophys. J.* **80,** 356A–356A
32. Palpant, N. J., Day, S. M., Herron, T. J., Converso, K. L., and Metzger, J. M. (2008) Single histidine-substituted cardiac troponin I confers protection from age-related systolic and diastolic dysfunction. *Cardiovasc. Res.* cvn198
33. Cho, M. C., Rapacciuolo, A., Koch, W. J., Kobayashi, Y., Jones, L. R., and Rockman, H. A. (1999) Defective beta-adrenergic receptor signaling precedes the development of dilated cardiomyopathy in transgenic mice with calsequestrin overexpression. *J. Biol. Chem.* **274,** 22251–22256
34. Davis, J., Wen, H., Edwards, T., and Metzger, J. M. (2007) Thin filament disinhibition by restrictive cardiomyopathy mutant R193H troponin I induces Ca^{2+}-independent mechanical tone and acute myocyte remodeling. *Circ. Res.* **100,** 1494–1502
35. Fentzke, R. C., Buck, S. H., Patel, J. R., Lin, H., Wolska, B. M., Stojanovic, M. O., Martin, A. F., Solaro, R. J., Moss, R. L., and Leiden, J. M. (1999) Impaired cardiomyocyte relaxation and diastolic function in transgenic mice expressing slow skeletal troponin I in the heart. *J. Physiol.* **517,** 143–157
36. Szatkowski, M. L., Westfall, M. V., Gomez, C. A., Wahr, P. A., Michele, D. E., DelloRusso, C., Turner, I. I., Hong, K. E., Albayya, F. P., and Metzger, J. M. (2001) In vivo acceleration of heart relaxation performance by parvalbumin gene delivery. *J. Clin. Invest.* **107,** 191–197
37. Michele, D. E., Gomez, C. A., Hong, K. E., Westfall, M. V., and Metzger, J. M. (2002) Cardiac dysfunction in hypertrophic cardiomyopathy mutant tropomyosin mice is transgene-dependent, hypertrophy-independent, and improved by beta-blockade. *Circ. Res.* **91,** 255–262
38. Whitesall, S. E., Hoff, J. B., Vollmer, A. P., and D'Alecy, L. G. (2004) Comparison of simultaneous measurement of mouse systolic arterial blood pressure by radiotelemetry and tail-cuff methods. *Am. J. Physiol. Heart Circ. Physiol.* **286,** H2408–H2415
39. Fu, Y., Huang, X., Zhong, H., Mortensen, R. M., D'Alecy, L. G., and Neubig, R. R. (2006) Endogenous RGS proteins and G-alpha subtypes differentially control muscarinic and adenosine-mediated chronotropic effects. *Circ. Res.* **98,** 659–666
40. Linder, A. E., Weber, D. S., Whitesall, S. E., D'Alecy, L. G., and Webb, R. C. (2005) Altered vascular reactivity in mice made hypertensive by nitric oxide synthase inhibition. *J. Cardiovasc. Pharmacol.* **46,** 438–444
41. Oldner, A., Konrad, D., Weitzberg, E., Rudehill, A., Rossi, P., and Wanecek, M. (2001) Effects of levosimendan, a novel inotropic calcium-sensitizing drug, in experimental septic shock. *Crit. Care Med.* **29,** 2185–2193
42. Ucgun, I., Oztuna, F., Dagli, C. E., Yildirim, H., and Bal, C. (2008) Relationship of metabolic alkalosis, azotemia and morbidity in patients with chronic obstructive pulmonary disease and hypercapnia. *Respiration* **276,** 270–274
43. Rocker, G. M., Mackenzie, M.-G., Williams, B., and Logan, P. M. (1999) Noninvasive positive pressure ventilation: successful outcome in patients with acute lung injury/ARDS. *Chest* **115,** 173–177
44. O'Croinin, D. F., Nichol, A. D., Hopkins, N., Boylan, J., O'Brien, S., O'Connor, C., Laffey, J. G., and McLoughlin, P. (2008) Sustained hypercapnic acidosis during pulmonary infection increases bacterial load and worsens lung injury. *Crit. Care Med.* **36,** 2128–2135
45. Harper, R. M., Macey, P. M., Woo, M. A., Macey, K. E., Keens, T. G., Gozal, D., and Alger, J. R. (2005) Hypercapnic exposure in congenital central hypoventilation syndrome reveals CNS respiratory control mechanisms. *J. Neurophysiol.* **93,** 1647–1658
46. Bers, D. M. (2002) Cardiac excitation-contraction coupling. *Nature* **415,** 198–205
47. Westfall, M. V., and Metzger, J. M. (2007) Single amino acid substitutions define isoform-specific effects of troponin I on myofilament Ca^{2+} and pH sensitivity. *J. Mol. Cell. Cardiol.* **43,** 107–118
48. Ricciardi, L., Bottinelli, R., Canepari, M., and Reggiani, C. (1994) Effects of acidosis on maximum shortening velocity and force-velocity relation of skinned rat cardiac muscle. *J. Mol. Cell. Cardiol.* **26,** 601–607
49. Ricciardi, L., Bucx, J. J., and ter Keurs, H. E. (1986) Effects of acidosis on force-sarcomere length and force-velocity relations of rat cardiac muscle. *Cardiovasc. Res.* **20,** 117–123
50. Tardiff, J. C., Hewett, T. E., Palmer, B. M., Olsson, C., Factor, S. M., Moore, R. L., Robbins, J., and Leinwand, L. A. (1999) Cardiac troponin T mutations result in allele-specific phenotypes in a mouse model for hypertrophic cardiomyopathy. *J. Clin. Invest.* **104,** 469–481
51. Arteaga, G. M., Warren, C. M., Milutinovic, S., Martin, A. F., and Solaro, R. J. (2005) Specific enhancement of sarcomeric response to Ca^{2+} protects murine myocardium against ischemia-reperfusion dysfunction. *Am. J. Physiol Heart Circ. Physiol.* **289,** H2183–H2192
52. Liou, Y. M., Kuo, S. C., and Hsieh, S. R. (2008) Differential effects of a green tea-derived polyphenol (-)-epigallocatechin-3-gallate on the acidosis-induced decrease in the Ca(2+) sensitivity of cardiac and skeletal muscle. *Pflügers Arch.* **456,** 787–800
53. Mann, D. L., and Bristow, M. R. (2005) Mechanisms and models in heart failure: the biomechanical model and beyond. *Circulation* **111,** 2837–2849
54. Sorsa, T., Pollesello, P., and Solaro, R. J. (2004) The contractile apparatus as a target for drugs against heart failure: interaction of levosimendan, a calcium sensitiser, with cardiac troponin C. *Mol. Cell. Biochem.* **266,** 87–107
55. Givertz, M. M., Andreou, C., Conrad, C. H., and Colucci, W. S. (2007) Direct myocardial effects of levosimendan in humans with left ventricular dysfunction: alteration of force-frequency and relaxation-frequency relationships. *Circulation* **115,** 1218–1224
56. Jorgensen, K., Bech-Hanssen, O., Houltz, E., and Ricksten, S. E. (2008) Effects of levosimendan on left ventricular relaxation and early filling at maintained preload and afterload conditions after aortic valve replacement for aortic stenosis. *Circulation* **117,** 1075–1081
57. Li, M. X., Spyracopoulos, L., and Sykes, B. D. (1999) Binding of Cardiac troponin-I147–163 induces a structural opening in human cardiac troponin-C. *Biochemistry* **38,** 8289–8298
58. Campbell, A. P., and Sykes, B. D. (1991) Interaction of troponin I and troponin C: Use of the two-dimensional nuclear magnetic resonance transferred nuclear overhauser effect to determine the structure of the inhibitory troponin I peptide when bound to skeletal troponin C. *J. Mol. Biol.* **222,** 405–421
59. Blumenschein, T. M. A., Tripet, B. P., Hodges, R. S., and Sykes, B. D. (2001) Mapping the interacting regions between troponins T and C. binding of TnT and TnI peptides to TnC and NMR mapping of the TnT-binding site on TnC. *J. Biol. Chem.* **276,** 36606–36612
60. Lindhout, D. A., and Sykes, B. D. (2003) Structure and dynamics of the C-domain of human cardiac troponin C in complex with the inhibitory region of human cardiac troponin I. *J. Biol. Chem.* **278,** 27024–27034
61. Takeda, S., Yamashita, A., Maeda, K., and Maeda, Y. (2003) Structure of the core domain of human cardiac troponin in the Ca^{2+}-saturated form. *Nature* **424,** 35–41

Received for publication September 15, 2008.
Accepted for publication December 4, 2008.